



GLOBAL JOURNAL OF MEDICAL RESEARCH: L  
NUTRITION & FOOD SCIENCE  
Volume 18 Issue 1 Version 1.0 Year 2018  
Type: Double Blind Peer Reviewed International Research Journal  
Publisher: Global Journals  
Online ISSN: 2249-4618 & Print ISSN: 0975-5888

## Evaluation of Consciousness Energy Healing Treated Pyridoxine (Vitamin B<sub>6</sub>)

By Dahryn Trivedi, Mahendra Kumar Trivedi, Alice Branton, Gopal Nayak & Snehasis Jana

*Trivedi Global, Inc. and Trivedi Science Research Laboratory Pvt. Ltd.*

**Abstract-** The aim of the research work to evaluate the impact of the Consciousness Energy Treatment on the physicochemical and thermal properties of pyridoxine using the modern analytical technique. The sample was divided into control and treated part. Only the treated sample was received the Trivedi Effect<sup>®</sup>-Consciousness Energy Treatment remotely by a renowned Biofield Energy Healer, Dahryn Trivedi. The particle sizes were significantly decreased by 17% (d<sub>10</sub>), 6.2% (d<sub>50</sub>), 0.54% (d<sub>90</sub>), and 0.3% {D(4,3)}; thus, the specific surface area was significantly increased by 13.72% in the treated pyridoxine compared with the control sample. The PXRD peak intensities and crystallite sizes were significantly altered ranging from -40.45% to 154.76% and -57% to 51.33%, respectively; however, the average crystallite size was decreased by 6.52% in the treated sample compared with the control sample. The heat requires to melt (fusion) the treated pyridoxine was increased by 3.82% compared with the control sample. The total weight loss was significantly decreased by 5.14%; however, the residue amount was significantly increased by 8.34% in the treated sample compared with the control sample.

**Keywords:** pyridoxine, the trivedi effect<sup>®</sup>, consciousness energy healing treatment, particle size, surface area, PXRD, DSC, TGA/DTG.

**GJMR-L Classification:** NLMC Code: QU 145



*Strictly as per the compliance and regulations of:*



© 2018. Dahryn Trivedi, Mahendra Kumar Trivedi, Alice Branton, Gopal Nayak & Snehasis Jana. This is a research/review paper, distributed under the terms of the Creative Commons Attribution-Noncommercial 3.0 Unported License (<http://creativecommons.org/licenses/by-nc/3.0/>), permitting all non-commercial use, distribution, and reproduction in any medium, provided the original work is properly cited.

# Evaluation of Consciousness Energy Healing Treated Pyridoxine (Vitamin B<sub>6</sub>)

Dahryn Trivedi <sup>α</sup>, Mahendra Kumar Trivedi <sup>σ</sup>, Alice Branton <sup>ρ</sup>, Gopal Nayak <sup>ω</sup> & Snehasis Jana <sup>¥</sup>

**Abstract-** The aim of the research work to evaluate the impact of the Consciousness Energy Treatment on the physicochemical and thermal properties of pyridoxine using the modern analytical technique. The sample was divided into control and treated part. Only the treated sample was received the Trivedi Effect<sup>®</sup>-Consciousness Energy Treatment remotely by a renowned Biofield Energy Healer, Dahryn Trivedi. The particle sizes were significantly decreased by 17%(d<sub>10</sub>), 6.2%(d<sub>50</sub>), 0.54%(d<sub>90</sub>), and 0.3% {D(4,3)}; thus, the specific surface area was significantly increased by 13.72% in the treated pyridoxine compared with the control sample. The PXRD peak intensities and crystallite sizes were significantly altered ranging from -40.45% to 154.76% and -57% to 51.33%, respectively; however, the average crystallite size was decreased by 6.52% in the treated sample compared with the control sample. The heat requires to melt (fusion) the treated pyridoxine was increased by 3.82% compared with the control sample. The total weight loss was significantly decreased by 5.14%; however, the residue amount was significantly increased by 8.34% in the treated sample compared with the control sample. The Trivedi Effect<sup>®</sup> might have generated a new polymorphic form of pyridoxine which may offer better solubility, bioavailability, and therapeutic efficacy against many diseases compared to the control sample.

**Keywords:** pyridoxine, the trivedi effect<sup>®</sup>, consciousness energy healing treatment, particle size, surface area, PXRD, DSC, TGA/DTG.

## I. INTRODUCTION

Pyridoxine is a water-soluble vitamin also known as vitamin B<sub>6</sub>. The active form of vitamin B<sub>6</sub> is pyridoxal 5'-phosphate, which functions as a coenzyme in many enzyme reactions in the proteins, lipids, carbohydrates metabolism, synthesis of neurotransmitters, and steroid hormones function<sup>[1]</sup>. Along with this, it also plays a significant role in the normal function of the nervous system, endocrine system, immune system, red blood cell, and also maintain the blood glucose level in the body<sup>[1-3]</sup>. Pyridoxine can be inter-converted into pyridoxal (aldehyde) and pyridoxamine (amine) form. Pyridoxine, pyridoxamine, and their phosphorylated forms are the major forms of vitamin B<sub>6</sub> in plant food, while pyridoxal and pyridoxal-5'-phosphate are obtained from animal food. The hydrochloride salt of vitamin B<sub>6</sub> is pyridoxine HCl<sup>[4]</sup>. Vitamin B<sub>6</sub> is commonly used as vitamin supplement or as a component of multivitamin

preparations to prevent and treat the vitamin B<sub>6</sub> deficiency, sideroblastic anaemia, pyridoxine dependency seizures, metabolic disorders, Alzheimer's disease, pulmonary tuberculosis, cardiovascular disease, hyperhomocysteinemia, anxiety, asthma, attention deficit hyperactivity disorder, cancer, depression, dysmenorrhoea, diabetes, post-partum lactation suppression, McArdle's disease, osteoporosis, etc.<sup>[2,5-8]</sup>. Vitamin B<sub>6</sub> is light sensitive and degrades slowly when exposed to light. It is soluble in water and alcohol; sparingly soluble in acetone; insoluble in ether and chloroform. When it heated to decomposition, it emits very toxic fumes of oxides of nitrogen and hydrogen chloride<sup>[9]</sup>.

Physicochemical properties of the pharmaceutical or nutraceutical compounds play a very crucial role in its dissolution, absorption, bioavailability, and therapeutic profile in the body<sup>[10]</sup>. In this regards, the Trivedi Effect<sup>®</sup>-Consciousness Energy Healing Treatment has a significant impact altering the physicochemical properties such as crystal structure, particle size, surface area, thermal behaviour, and bioavailability profile of pharmaceutical and nutraceutical compounds<sup>[11-14]</sup>. The Trivedi Effect<sup>®</sup> is a natural and only scientifically proven phenomenon in which an expert can harness this inherently intelligent energy from the Universe and transmit it anywhere on the planet through the possible mediation of neutrinos<sup>[15]</sup>. The Biofield is a unique, infinite, and para-dimensional electromagnetic energy field exists surrounding the body of every living organism, which is generated from the continuous moment of charged particles (i.e., ions, cells, blood flow, etc.) inside the body. The Biofield based Energy Healing Therapies have significant beneficial outcomes against various disease conditions<sup>[16]</sup>. The National Institutes of Health/National Center for Complementary and Alternative Medicine (NIH/NCCAM) recommend and included the Energy therapy under Complementary and Alternative Medicine (CAM) category along with other therapies, i.e., homeopathy, naturopathy, Ayurvedic medicine, acupuncture, acupressure, Qi Gong, Tai Chi, Reiki, healing touch, Rolfing, hypnotherapy, etc., which have been accepted by most of the USA people<sup>[17,18]</sup>. The Trivedi Effect<sup>®</sup>-Consciousness Energy Healing Treatment also has the significant impact on the properties of metals, ceramics, and polymers, organic compounds, microorganisms, cancer cell, and improve

Author <sup>α σ ρ ω</sup>: Trivedi Global, Inc., Henderson, USA.

Author <sup>¥</sup>: Trivedi Science Research Laboratory Pvt. Ltd., Bhopal, India.  
e-mail: publication@trivedisrl.com

the overall productivity of crops<sup>[19-28]</sup>. All these outstanding results inspired the authors to evaluate the impact of the Trivedi Effect®-Consciousness Energy Healing Treatment on the behavioural, physicochemical, and thermal properties of pyridoxine HCl using powder particle size analysis (PSA), X-ray diffraction (PXRD), differential scanning calorimetry (DSC), and thermogravimetric analysis (TGA)/differential thermogravimetric analysis (DTG).

## II. MATERIALS AND METHODS

### a) Chemicals and Reagents

Pyridoxine HCl was purchased from Tokyo Chemical Industry Co. Ltd., Japan. All other chemicals utilized in the experiments were of analytical grade available in India.

### b) Consciousness Energy Healing Treatment Strategies

The pyridoxine powder sample was divided into two equal parts. One part of pyridoxine was treated with the Trivedi Effect®-Consciousness Energy Healing Treatment remotely under standard laboratory conditions for 3 minutes by the renowned Biofield Energy Healer, Dahryn Trivedi, USA, and known as a treated sample. However, the second part of the test sample did not receive the Biofield Energy Treatment and termed as a control sample. The control sample later received the treatment from a "sham" healer, whereas the "sham" healer was ignorant about the Biofield Energy Treatment. After the treatment, the Biofield Energy Treated and untreated samples were kept in sealed conditions and characterized using PSA, PXRD, DSC, and TGA analytical techniques.

### c) Characterization

The PSA, PXRD, DSC, and TGA analysis of pyridoxine were performed. The PSA was performed using Malvern Master sizer 2000, from the UK with a detection range between 0.01  $\mu\text{m}$  to 3000  $\mu\text{m}$  using the wet method<sup>[28,29]</sup>. The PXRD analysis of pyridoxine powder sample was performed with the help of Rigaku MiniFlex-II Desktop X-ray diffractometer (Japan)<sup>[31,32]</sup>. The average size of crystallites was calculated from PXRD data using the Scherrer's formula (1):

$$G = k\lambda/\beta\cos\theta \quad (1)$$

Where G is the crystallite size in nm, k is the equipment constant (0.94),  $\lambda$  is the radiation wavelength (0.154056 nm for K $\alpha$ 1 emission),  $\beta$  is the full-width at half maximum, and  $\theta$  is the Bragg angle<sup>[33]</sup>.

Similarly, the DSC analysis of pyridoxine was performed with the help of DSC Q200, TA instruments<sup>[28,29]</sup>. The TGA/DTG thermograms of pyridoxine were obtained with the help of TGA Q50TA instruments<sup>[28,29]</sup>.

The % change in particle size, specific surface area (SSA), peak intensity, crystallite size, melting point, latent heat, weight loss and the maximum thermal degradation temperature ( $T_{\text{max}}$ ) of the Biofield Energy Treated sample was calculated compared with the control sample using the following equation 2:

$$\% \text{ change} = \frac{[\text{Treated} - \text{Control}]}{\text{Control}} \times 100 \quad (2)$$

## III. RESULTS AND DISCUSSION

### a) Particle Size Analysis (PSA)

The particle size analysis of both the control and the Biofield Energy Treated pyridoxine powder samples were performed, and the data are presented in Table 1. The particle sizes in the Biofield Energy Treated sample were significantly decreased at  $d_{10}$ ,  $d_{50}$ ,  $d_{90}$ , and D(4,3) by 17%, 6.2%, 0.54%, and 0.3% respectively compared to the control sample. However, the particle size value in the Biofield Energy Treated pyridoxine was significantly increased at by compared to the control sample. The SSA of the Biofield Energy Treated pyridoxine (0.456  $\text{m}^2/\text{g}$ ) was significantly increased by 13.72% compared to the control sample (0.401  $\text{m}^2/\text{g}$ ). From the results, it can be assumed that the Biofield Energy Healing Treatment acting as an external force for breaking the larger particles to smaller one in size, hence increased the surface area. The particle size, shape, and surface area have their impact on the solubility, dissolution rate, absorption, bioavailability, and therapeutic efficacy of a drug<sup>[34,35]</sup>. Thus, the Biofield Energy Treated pyridoxine would assume to enhance the therapeutic efficacy of the nutraceutical and pharmaceutical formulations.

Table 1: Particle Size Distribution of the Control and Biofield Energy Treated Pyridoxine

Parameter	$d_{10}$ ( $\mu\text{m}$ )	$d_{50}$ ( $\mu\text{m}$ )	$d_{90}$ ( $\mu\text{m}$ )	D(4,3) ( $\mu\text{m}$ )	SSA ( $\text{m}^2/\text{g}$ )
Control	8.22	40.38	138.77	60.44	0.401
Biofield Treated	6.82	37.88	138.02	60.26	0.456
Percent Change* (%)	-17.00	-6.20	-0.54	-0.30	13.72

$d_{10}$ ,  $d_{50}$ , and  $d_{90}$ : particle diameter corresponding to 10%, 50%, and 90% of the cumulative distribution, D(4,3): the average mass-volume diameter, and SSA: the specific surface area. \*denotes the percentage change in the Particle size distribution of the treated sample with respect to the control sample.

### b) Powder X-ray Diffraction (PXRD) Analysis

The PXRD diffractograms of the control and treated pyridoxine showed sharp and intense (Figure 1)

indicated that both the samples were crystalline. The control and Biofield Energy Treated pyridoxine powder samples showed the highest peak intensity at  $2\theta$  equal

to 25° (Table 2, entry 7). The peak intensities of the Biofield Energy Treated pyridoxine sample were significantly altered ranging from -40.45% to 154.76% compared to the control sample.

Table 2: PXRD Data for the Control and the Treated Pyridoxine

Entry No.	Bragg Angle (°2θ)		Peak Intensity (%)			Crystallite Size (G, nm)		
	Control	Treated	Control	Treated	% Change <sup>a</sup>	Control	Treated	% Change <sup>b</sup>
1	10.28	10.33	157.00	129.00	-17.83	344.00	307.00	-10.76
2	15.49	15.56	22.00	20.00	-9.09	362.00	443.00	22.38
3	16.86	16.93	65.00	57.00	-12.31	353.00	301.00	-14.73
4	18.61	18.65	39.00	30.00	-23.08	393.00	444.00	12.98
5	20.72	20.75	962.00	899.00	-6.55	413.00	440.00	6.54
6	24.10	24.09	63.00	94.00	49.21	386.00	498.00	29.02
7	25.00	25.04	1301.00	1292.00	-0.69	429.00	437.00	1.86
8	25.77	25.78	117.00	110.00	-5.98	306.00	317.00	3.59
9	27.77	27.81	1025.00	1075.00	4.88	431.00	422.00	-2.09
10	28.86	28.91	125.00	121.00	-3.20	149.00	143.00	-4.03
11	31.34	31.44	25.00	16.00	-36.00	529.00	277.00	-47.64
12	33.63	33.71	42.00	107.00	154.76	380.00	223.00	-41.32
13	37.09	37.20	89.00	53.00	-40.45	261.00	338.00	29.50
14	37.63	37.74	28.00	51.00	82.14	393.00	169.00	-57.00
15	38.55	38.49	42.00	39.00	-7.14	134.00	78.00	-41.79
16	47.32	47.36	41.00	44.00	7.32	150.00	227.00	51.33
17	53.26	53.30	137.00	160.00	16.79	259.00	238.00	-8.11
18	Average Crystallite Size					333.65	311.88	-6.52

<sup>a</sup> denotes the percentage change in the peak intensity of the Biofield Energy Treated sample with respect to the control sample; <sup>b</sup> denotes the percentage change in the crystallite size of the Biofield Energy Treated sample with respect to the control sample.

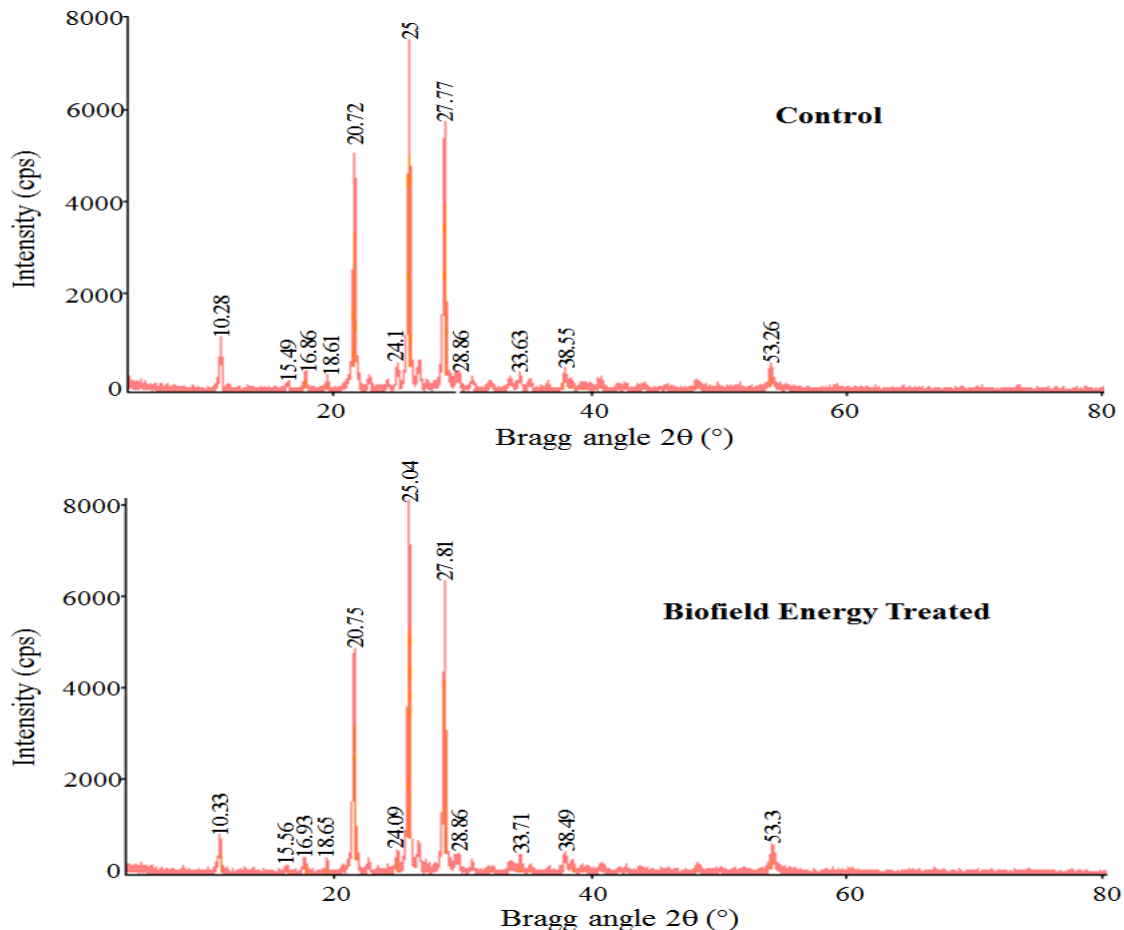


Fig. 1: PXRD Diffractograms of the Control and Biofield Energy Treated Pyridoxine

Similarly, the crystallite sizes of the Biofield Energy Treated pyridoxine powder sample were significantly altered ranging from -57% to 51.33% compared to the control sample. Overall, the average crystallite size of the Biofield Energy Treated pyridoxine powder sample (311.88 nm) was significantly decreased by 6.52% compared with the control sample (333.65 nm).

The peak intensities and crystallite sizes of the Biofield Energy Treated pyridoxine powder samples were significantly altered compared to the control sample. The peak intensity of each diffraction face of a compound changes according to the change in the crystal morphology<sup>[36]</sup> and alterations in the PXRD pattern provide the proof of polymorphic transitions<sup>[37,38]</sup>. The Biofield Energy Healing Treatment probably produced the new polymorphic form of pyridoxine through the Biofield Energy *via* neutrino oscillations<sup>[14]</sup>.

Different polymorphic forms of the pharmaceuticals have significant effects on the drug performance, because of their different thermodynamic and physicochemical properties from the original one<sup>[39,40]</sup>. Therefore, it is assumed that the Trivedi Effect®-Consciousness Energy Healing Treated pyridoxine would be better in designing novel pharmaceutical formulations for more drug performance.

### c) Differential Scanning Calorimetry (DSC) Analysis

The DSC thermograms of both the control and Biofield Energy Treated pyridoxine samples showed a very sharp endothermic peak at 215.42°C and 215.2°C, respectively (Figure 2). The experimental results closely matched to the reported data<sup>[41]</sup>. The melting point of the Biofield Energy Treated pyridoxine did not alter much compared to the control sample (Table 3).

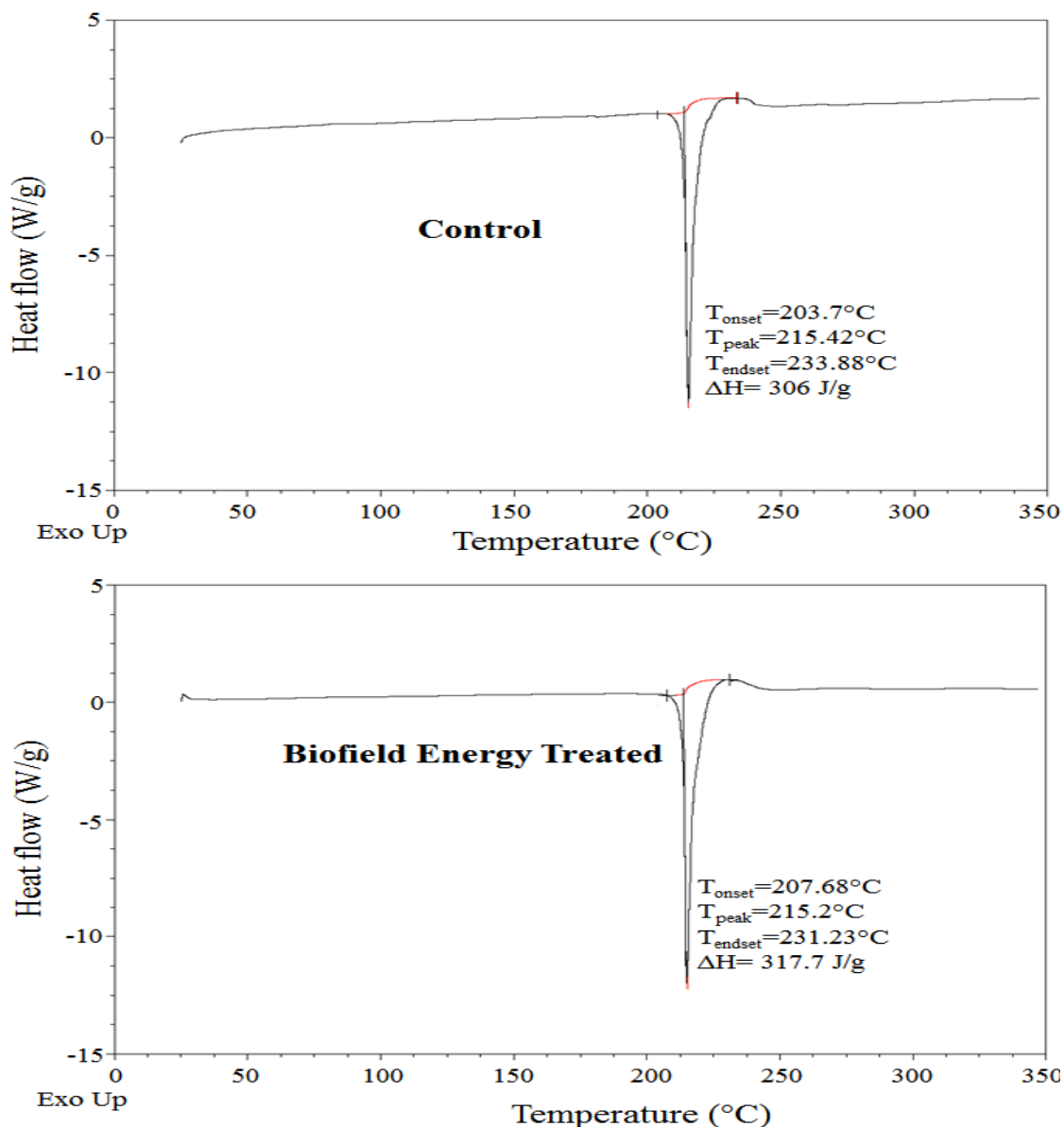


Fig. 2: DSC Thermograms of the Control and Biofield Energy Treated Pyridoxine



**Table 3:** DSC Data for Both Control and Biofield Energy Treated Samples of Pyridoxine

Sample	Melting Temp (°C)	$\Delta H_{\text{Fusion}}$ (J/g)
Control Sample	215.42	306.00
Biofield Energy Treated	215.20	317.70
% Change*	-0.10	3.82

$\Delta H$ : Latent heat of fusion, \*denotes the percentage change of the Biofield Energy Treated pyridoxine with respect to the control sample.

The latent heat of fusion ( $\Delta H_{\text{fusion}}$ ) of the Biofield Energy Treated sample (317.7 J/g) was increased by 3.82% compared with the control sample (306 J/g) (Table 3). Any change in the latent heat of fusion can be attributed to the disrupted molecular chains and the crystal structure of that compound<sup>[42]</sup>. Therefore, the Trivedi Effect® - Consciousness Energy Healing Treatment assumed to have a significant impact on the molecular chains and crystal structure of the treated pyridoxine responsible for the elevation of thermal stability compared to the control sample.

d) *Thermal Gravimetric Analysis (TGA)/ Differential Thermogravimetric Analysis (DTG)*

The TGA thermograms of both the control and Biofield Energy Treated pyridoxine samples showed two steps of thermal degradation (Figure 3). The total weight loss of the Biofield Energy Treated sample was significantly decreased by 5.14% compared to the control sample. Thus, the residue amount was

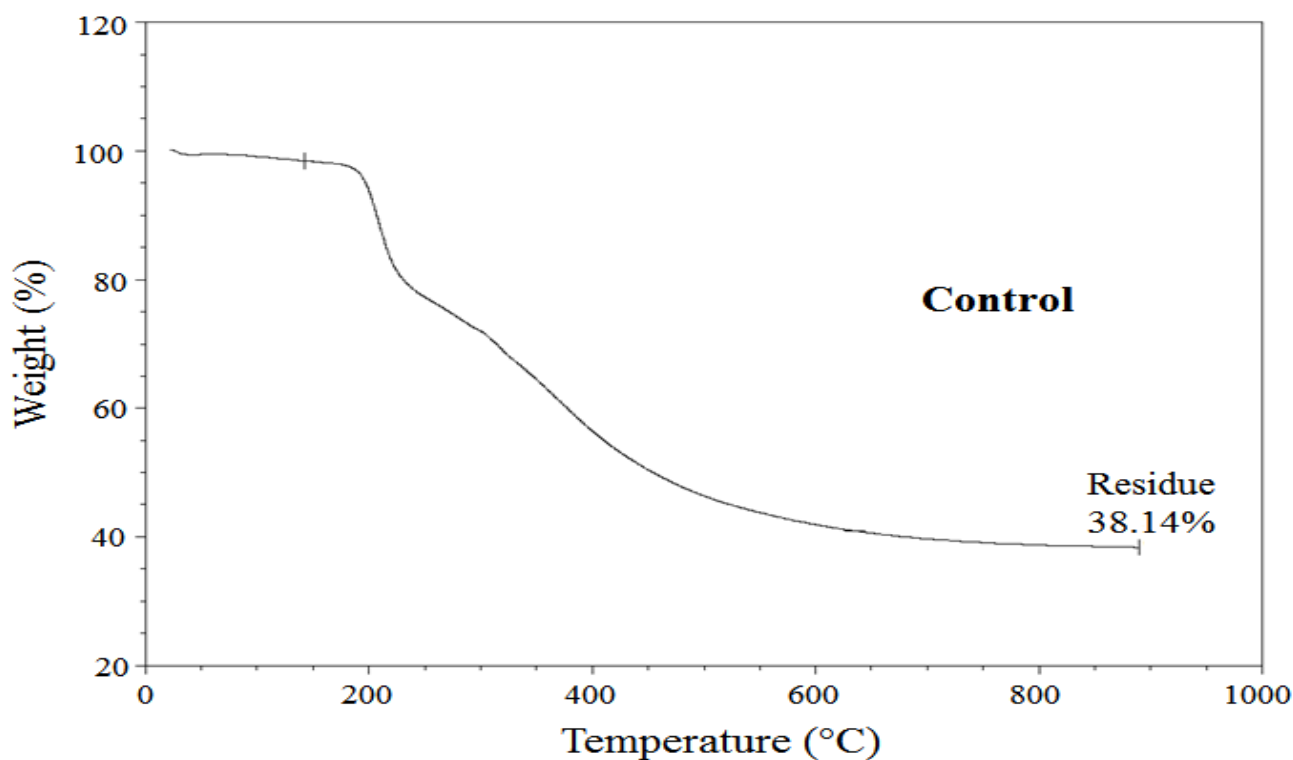
significantly increased by 8.34% in the Biofield Energy Treated pyridoxine compared to the control sample (Table 4).

**Table 4:** TGA/DTG Data of the Control and Biofield Energy Treated Samples of Pyridoxine

Sample	TGA		DTG; $T_{\text{max}}$ (°C)	
	Total Weight Loss (%)	Residue %	1 <sup>st</sup> Peak	2 <sup>nd</sup> Peak
Control	61.86	38.14	208.75	381.08
Biofield Energy Treated	58.68	41.32	214.94	373.16
% Change*	-5.14	8.34	2.97	-2.08

\* denotes the percentage change of the Biofield Energy Treated sample with respect to the control sample,  $T_{\text{max}}$  = the temperature at which maximum weight loss takes place in TG or peak temperature in DTG.

The DTG thermograms of the control and Biofield Energy Treated pyridoxine also reported two peaks in the thermograms (Figure 4). The  $T_{\text{max}}$  of the 1st peak of the Biofield Energy Treated sample was increased by 2.97%, whereas  $T_{\text{max}}$  of 2nd peak was decreased by 2.08% compared to the control sample (Table 4). Overall, TGA/DTG analysis revealed that the thermal stability of the Biofield Energy Treated sample was significantly increased compared with the control sample.



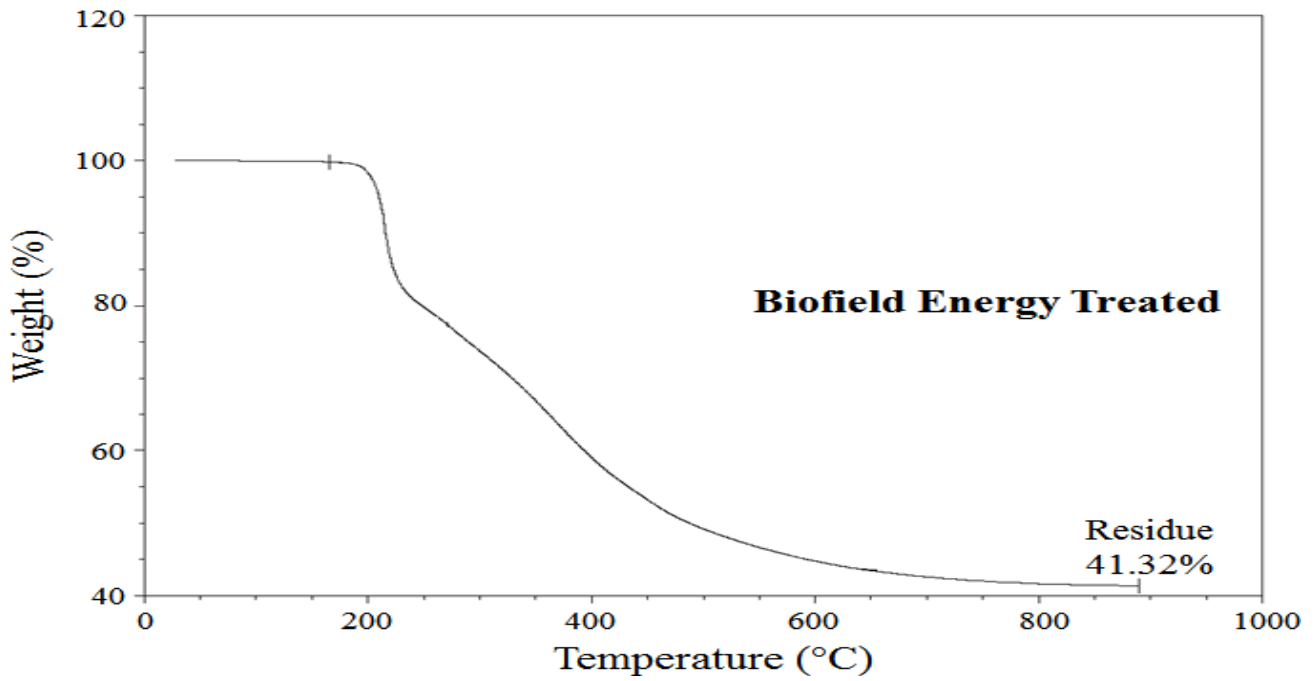


Fig. 3: TGA Thermograms of the Control and Biofield Energy Treated Pyridoxine

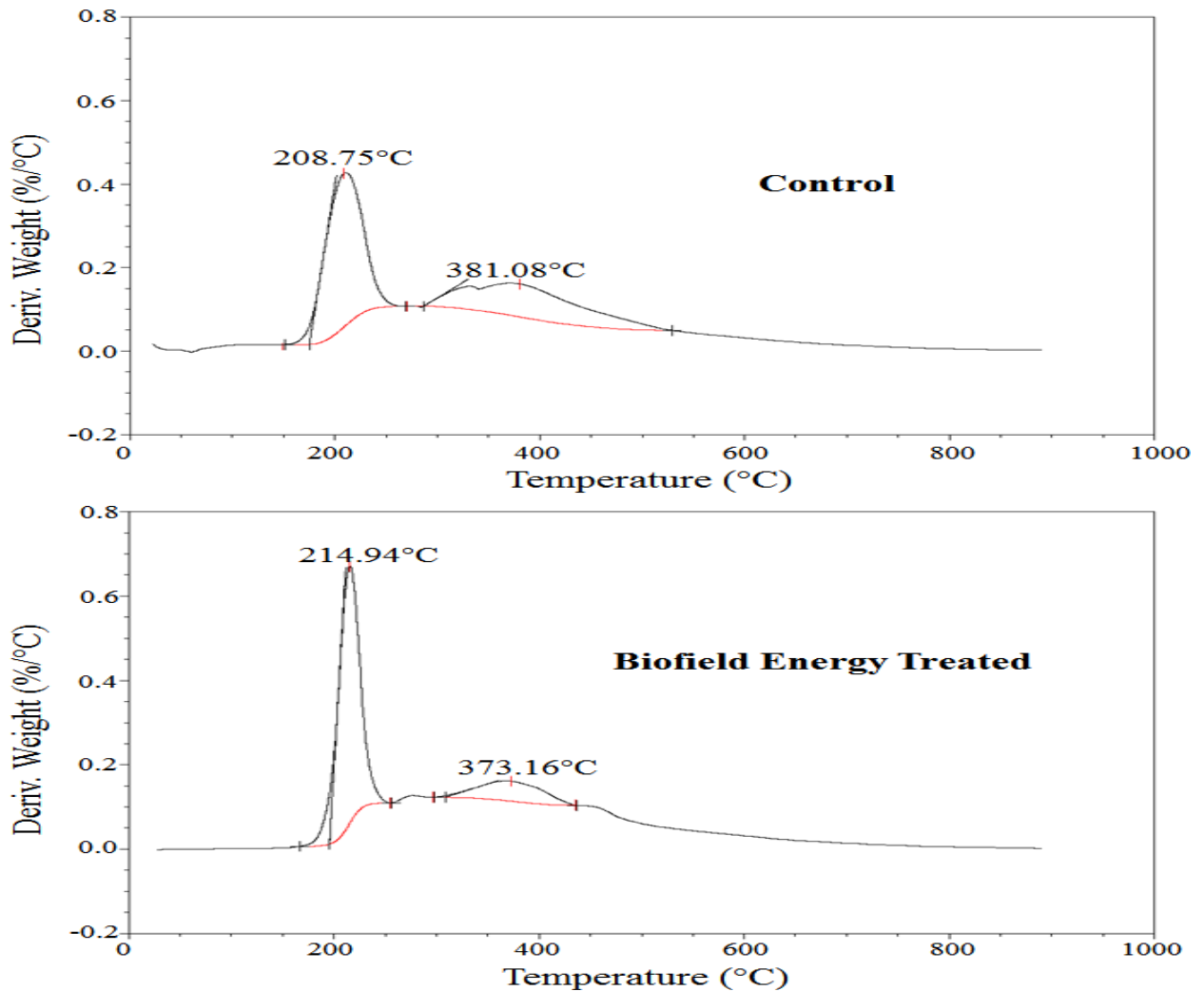


Fig. 4: DTG Thermograms of the Control and Biofield Energy Treated Pyridoxine

## IV. CONCLUSIONS

The Trivedi Effect<sup>®</sup>-Consciousness Energy Healing Treatment has shown a significant effect on the crystallite size, particle size, SSA, and thermal behavior of pyridoxine. The particle sizes in the Biofield Energy Treated powder sample was significantly decreased by 17%, 6.2%, 0.54%, and 0.3% at  $d_{10}$ ,  $d_{50}$ ,  $d_{90}$ , and  $D(4,3)$  respectively, compared to the control sample. Therefore, the SSA of the Biofield Energy Treated sample was significantly increased by 13.72% compared to the control sample. The PXRD peak intensities and crystallite sizes of the treated pyridoxine were significantly altered ranging from -40.45% to 154.76% and -57% to 51.33%, respectively compared to the control sample. The average crystallite size of the Biofield Energy Treated pyridoxine was significantly decreased by 6.52% compared with the control sample. The  $\Delta H_{\text{fusion}}$  was increased by 3.82% in the Biofield Energy Treated sample compared with the control sample. The total weight loss was significantly decreased by 5.14%; hence the residue amount was significantly increased by 8.34% in the Biofield Energy Treated sample compared with the control sample. From the results, it is concluded that the Trivedi Effect<sup>®</sup>-Consciousness Energy Healing Treatment might have generated a new polymorphic form of pyridoxine which may offer better solubility, bioavailability, and therapeutic efficacy compared with the control sample. The Trivedi Effect<sup>®</sup>-Consciousness Energy Healing Treated pyridoxine hydrochloride would be very useful to design novel pharmaceutical and nutraceutical formulations that may offer better therapeutic response against vitamin B<sub>6</sub> deficiency, pyridoxine-dependency seizures, sideroblastic anemia, Alzheimer's disease, metabolic disorders, diabetes, pulmonary tuberculosis, cardiovascular disease, hyperhomocysteinemia, cancer, anxiety, asthma, depression, attention deficit hyperactivity disorder (ADHD), dysmenorrhoea, post-partum lactation suppression, McArdle's disease, osteoporosis, etc.

## ACKNOWLEDGEMENTS

The authors are grateful to Central Leather Research Institute, SIPRA Lab. Ltd., Trivedi Science, Trivedi Global, Inc., Trivedi Testimonials, and Trivedi Master Wellness for their assistance and support during this work.

### Abbreviations

DSC: Differential scanning calorimetry,

FWHM: Full width half maximum.

G: Crystallite size.

$T_{\text{onset}}$ : Onset decomposition temperature.

$T_{\text{peak}}$ : Peak decomposition temperature.

$T_{\text{endset}}$ : Endset decomposition temperature.

$\Delta H$ : Enthalpy of fusion/decomposition.

PSA: Particle size distribution analysis.

PXRD: Powder X-ray diffraction.

TGA: Thermal gravimetric analysis.

SSA: Specific surface area.

DTG: Differential thermogravimetric analysis.

NIH: National institutes of health.

NCCAM: National center for complementary and alternative medicine.

CAM: Complementary and alternative medicine.

## REFERENCES RÉFÉRENCES REFERENCIAS

1. Vitamin-B<sub>6</sub>. (2018, August 7). Retrieved from: <https://ipi.oregonstate.edu/mic/vitamins/vitamin-B6>.
2. Dakshinamurti S, Dakshinamurti K (2007) Vitamin B<sub>6</sub> in Handbook of Vitamins, 4th Edn., Zempleni J, Rucker RB, McCormick DB, Suttie JW, CRC Press, Taylor & Francis Group, Boca Raton, USA, PP. 315-360.
3. Pyridoxine. (2018, August 7). Retrieved from: <https://en.wikipedia.org/wiki/Pyridoxine>.
4. Aboul-Enein H. Y, Loutfy M. A (1984) Pyridoxine Hydrochloride in Analytical Profiles of Drug Substances, Florey K (Ed.), Vol 13, Academic Press, Inc., Orlando, USA, PP. 448-478.
5. Leklem J. E (2001) Vitamin B<sub>6</sub> in Handbook of Vitamins, 3<sup>rd</sup> Edn., Rucker R. B, Suttie J. W, McCormick D. B, Machlin L. J, Marcel Dekker, Inc., New York, PP. 339-396.
6. The Many Uses for Vitamin B<sub>6</sub>. (2018, August 7). Retrieved from: <http://www.naturalmedicinejournal.com/journal/2011-09/many-uses-vitamin-b6>.
7. Qian B, Shen S, Zhang J, et al. Effects of Vitamin B<sub>6</sub> deficiency on the composition and functional potential of T cell populations. J Immunol Res 2017: 2197975.
8. AlSaad D, Awaisu A, Elsalem S, et al. Is pyridoxine effective and safe for post-partum lactation inhibition? A systematic review. J Clin Pharm Ther 2017: doi: 10.1111/jcpt.12526.
9. Pyridoxine Hydrochloride. (2018, August 7). Retrieved from: [https://pubchem.ncbi.nlm.nih.gov/compound/pyridoxine\\_hydrochloride#section=Stability](https://pubchem.ncbi.nlm.nih.gov/compound/pyridoxine_hydrochloride#section=Stability).
10. Cheron R (2009) Bioavailability, bioequivalence, and drug selection. In: Makoid CM, Vuchetich P. J, Banakar U. V (Eds) Basic pharmacokinetics (1<sup>st</sup> Edn.) Pharmaceutical Press, London.
11. Trivedi M. K, Branton A, Trivedi D, et al. Spectroscopic characterization of disulfiram and nicotinic acid after biofield treatment. J Anal Bioanal Tech 2015: 6: 265.
12. Trivedi M. K, Tallapragada R. M, Branton A, et al. Evaluation of biofield energy treatment on physical and thermal characteristics of selenium powder. Journal of Food and Nutrition Sciences 2015: 3: 223-228.



13. Branton A, Jana S. The influence of energy of consciousness healing treatment on low bioavailable resveratrol in male Sprague Dawley rats. *International Journal of Clinical and Developmental Anatomy* 2017; 3: 9-15.
14. Branton A, Jana S. Effect of The biofield energy healing treatment on the pharmacokinetics of 25-hydroxyvitamin D<sub>3</sub> [25(OH)D<sub>3</sub>] in rats after a single oral dose of vitamin D<sub>3</sub>. *American Journal of Pharmacology and Phytotherapy* 2017; 2: 11-18.
15. Trivedi M. K, Mohan T. R. R. Biofield energy signals, energy transmission and neutrinos. *American Journal of Modern Physics* 2016; 5: 172-176.
16. Rubik B, Muehsam D, Hammerschlag R, et al. Biofield science and healing: history, terminology, and concepts. *Glob Adv Health Med* 2015; 4: 8-14.
17. Barnes P. M, Bloom B, Nahin R. L. Complementary and alternative medicine use among adults and children: United States, 2007. *Natl Health Stat Report* 2008; 12: 1-23.
18. Koithan M. Introducing complementary and alternative therapies. *J Nurse Prac* 2009; 5: 18-20.
19. Trivedi M. K, Nayak G, Patil S, et al. Characterization of physical and structural properties of brass powder after biofield treatment. *J Powder Metall Min* 2015; 4: 134.
20. Trivedi M. K, Nayak G, Patil S, et al. Studies of the atomic and crystalline characteristics of ceramic oxide nano powders after bio field treatment. *Ind Eng Manage* 2015; 4: 161.
21. Trivedi M. K, Nayak G, Patil S, et al. Influence of biofield treatment on physicochemical properties of hydroxyethyl cellulose and hydroxypropyl cellulose. *J Mol Pharm Org Process Res* 2015; 3: 126.
22. Trivedi M. K, Branton A, Trivedi D, et al. Gas chromatography-mass spectrometric analysis of isotopic abundance of <sup>13</sup>C, <sup>2</sup>H, and <sup>18</sup>O in biofield energy treated p-tertiary butylphenol (PTBP). *American Journal of Chemical Engineering* 2016; 4: 78-86.
23. Trivedi M. K, Branton A, Trivedi D, et al. Gas chromatography-mass spectrometry based isotopic abundance ratio analysis of biofield energy treated methyl-2-naphthylether (Nerolin). *American Journal of Physical Chemistry* 2016; 5: 80-86.
24. Trivedi MK, Branton A, Trivedi D, et al. Antimicrobial sensitivity, biochemical characteristics and biotyping of *Staphylococcus saprophyticus*: An impact of biofield energy treatment. *J Women's Health Care* 2015; 4: 271.
25. Trivedi M. K, Branton A, Trivedi D, et al. Antibioigram of multidrug-resistant isolates of *Pseudomonas aeruginosa* after biofield treatment. *J Infect Dis Ther* 2015; 3: 244.
26. Trivedi M. K, Patil S, Shettigar H, et al. The potential impact of biofield treatment on human brain tumor cells: A time-lapse video microscopy. *J Integr Oncol* 2015; 4: 141.
27. Trivedi M. K, Branton A, Trivedi D, et al. Evaluation of plant growth, yield and yield attributes of biofield energy treated mustard (*Brassica juncea*) and chick pea (*Cicer arietinum*) seeds. *Agriculture, Forestry and Fisheries* 2015; 4: 291-295.
28. Trivedi M. K, Branton A, Trivedi D, et al. Evaluation of vegetative growth parameters in biofield treated bottle gourd (*Lagenaria siceraria*) and okra (*Abelmoschus esculentus*). *International Journal of Nutrition and Food Sciences* 2015; 4: 688-694.
29. Trivedi M. K, Sethi K. K, Panda P, et al. A comprehensive physicochemical, thermal, and spectroscopic characterization of zinc (II) chloride using X-ray diffraction, particle size distribution, differential scanning calorimetry, thermogravimetric analysis/differential thermogravimetric analysis, ultraviolet-visible, and Fourier transform-infrared spectroscopy. *International Journal of Pharmaceutical Investigation* 2017; 7: 33-40.
30. Trivedi M. K, Sethi K. K, Panda P, et al. Physicochemical, thermal and spectroscopic characterization of sodium selenate using XRD, PSD, DSC, TGA/DTG, UV-vis, and FT-IR. *Marmara Pharmaceutical Journal* 2017; 21/2: 311-318.
31. Desktop X-ray Diffractometer "MiniFlex+". *The Rigaku Journal* 1997; 14: 29-36.
32. Zhang T, Paluch K, Scalabrino G, et al. Molecular structure studies of (1S,2S)-2-benzyl-2,3-dihydro-2-(1Hinden-2-yl)-1H-inden-1-ol. *J Mol Struct* 2015; 1083: 286-299.
33. Langford J. I, Wilson A. J. C. Scherrer after sixty years: A survey and some new results in the determination of crystallite size. *J Appl Cryst.* 1978; 11: 102-113.
34. Chereson R. (2009) Bioavailability, bioequivalence, and drug selection. In: Makoid C. M, Vuchetich P. J, Banakar U. V (eds) *Basic pharmacokinetics* (1<sup>st</sup> Edn.) Pharmaceutical Press, London.
35. Khadka P, Ro J, Kim H, et al. Pharmaceutical particle technologies: An approach to improve drug solubility, dissolution and bioavailability. *Asian J Pharm Sci* 2014; 9: 304-316.
36. Raza K, Kumar P, Ratan S, et al. Polymorphism: The phenomenon affecting the performance of drugs. *SOJ Pharm Pharm Sci* 2014; 1: 10.
37. Brittain H. G. (2009) *Polymorphism in pharmaceutical solids in Drugs and Pharmaceutical Sciences*, Volume 192, 2<sup>nd</sup> Edn., Informa Healthcare USA, Inc., New York.
38. Censi R, Martino P. D. Polymorph impact on the bioavailability and stability of poorly soluble drugs. *Molecules* 2015; 20: 18759-18776.
39. Blagden N, de Matas M, Gavan P. T, et al. Crystal engineering of active pharmaceutical ingredients to

- improve solubility and dissolution rates. *Adv Drug Deliv Rev* 2007; 59: 617-630.
40. Cherson R. (2009) Bioavailability, bioequivalence, and drug selection. In: Makoid C. M, Vuchetich P. J, Banakar U. V (eds) *Basic pharmacokinetics* (1<sup>st</sup> Edn.) Pharmaceutical Press, London.
  41. Han D, Li X, Wang H, et al. Determination and correlation of pyridoxine hydrochloride solubility in different binary mixtures at temperatures from (278.15 to 313.15) K. *J Chem Thermodyn* 2016; 94: 138-151.
  42. Zhao Z, Xie M, Li Y, et al. Formation of curcumin nanoparticles *via* solution-enhanced dispersion by supercritical CO<sub>2</sub>. *Int J Nanomedicine* 2015; 10: 3171-3181.





This page is intentionally left blank